Geothermics 84 (2020) 101738

Contents lists available at ScienceDirect

Geothermics

journal homepage: www.elsevier.com/locate/geothermics

Hydrogeochemical characteristics at Doña Juana Complex (SW Colombia): A new area for geothermal exploration in the Northern Andes region

Esteban Gómez Diaz[a,*], Maria I. Marín Cerón[b]

[a] Iceland School of Energy, Reykjavik University, Iceland
[b] Department of Earth Sciences, EAFIT University, Colombia

ARTICLE INFO

Keywords:
Geothermal exploration
Geothermal Colombia
Doña Juana Complex
Hydrogeochemical
Geothermometry
High temperature system

ABSTRACT

The Doña Juana Volcanic Complex (DJVC) is an active volcanic zone located in southern Colombia, an area lacking geothermal exploration data. Using the results of hydrogeochemical analyses of hot springs, thermal waters were divided into two groups: Doña Juana System (DJS) and Las Animas System (AS). The DJS thermal waters are sulphate-bicarbonate and the AS dilute-chloride waters with relatively high concentrations of alkalis. The stable isotope and some element ratios suggested a mixing process between geothermal fluids and meteoric waters where AS is related to the upflow with a reservoir temperature around 180 °C estimated through solute geothermometers and mineral equilibrium geothermometry, showing a high temperature system in which the fault systems apparently play an important role in the flow of the geothermal fluids.

1. Introduction

The most important geothermal exploration studies in Colombia have been carried out in the following systems: 1) Nevado del Ruiz, which is probably the best known geothermal zone in Colombia due to the inter-government and private cooperation (Colombian Geological Survey, National Univesity of Colombia and the most important hydropower companies CHEC- EPM and ISAGEN); 2) Tufiño Volcanic Complex - Chiles - Cerro Negro, in which there is a bi-national project between Ecuador and Colombia; 3) Azufral Volcano, 4) Paipa and recently 5) the San Diego Volcano area. The Colombia Geological Survey (SGC by its abbreviation in Spanish) has recently studied these last three. However, there are unexplored areas such as the Doña Juana Volcanic Complex (DJVC).

The DJVC is a volcanic complex located in the southern Colombian Central Cordillera between the departments of Nariño, Cauca and Putumayo (Fig. 1). It presents favorable characteristics for geothermal studies such as hydrothermal manifestations (e.g. hot springs with temperatures ranging from 24°C to 69°C and pH values between 5,75 and 6,70) and, a favorable structurall setting associated with a caldera-type volcano.

This paper is looking for an understanding the hydrochemistry of thermal waters by studying the concentrations of dissolved ions and the ratios of stable isotopes with the aim of identifying associations with various parts of the geothermal system. Different plots and element relationships were used to characterize the thermal waters. To infer the temperatures at depth, the geothermometer techniques such as a solute geothermometer based on empirical analytical equations and chemical reactions between the geothermal fluid and minerals at depth were used.

Furthermore, the mineral equilibria geothermometry was used to identify mineral equilibrium to correlate and compare with the geothermometers. This can be used to generate possible equilibria between aqueous solution components and minerals (Pang and Reed, 1988). For mineral equilibrium geothermometry it was necessary to calculate the saturation index (SI) defined as Log Q/K; the values are obtained from the log of solubility products of the minerals in the water, where Q is the calculated ion activity product in the water and K is the equilibrium constant (Eq. 1). We determined whether the water in contact with the minerals was in chemical equilibrium with respect to these minerals (SI = 0), or under-saturated (SI < 0; mineral dissolution can occur) or over-saturated (SI > 0; mineral precipitation is possible).

$$\text{Saturation index (SI)} = \log (Q/K) \quad (1)$$

Nevertheless, the mineral equilibrium geothermometry can exhibit signs of mixing because dilution and boiling may alter the results and hence the values of Q and K, as well as the slopes of the saturation curves, thereby leading to erroneous interpretations of the different samples (Reed and Spycher, 1984).

* Corresponding author.
E-mail address: esteban18@ru.is (E. Gómez Diaz).

https://doi.org/10.1016/j.geothermics.2019.101738
Received 17 August 2017; Received in revised form 13 September 2019; Accepted 26 September 2019
Available online 15 October 2019
0375-6505/

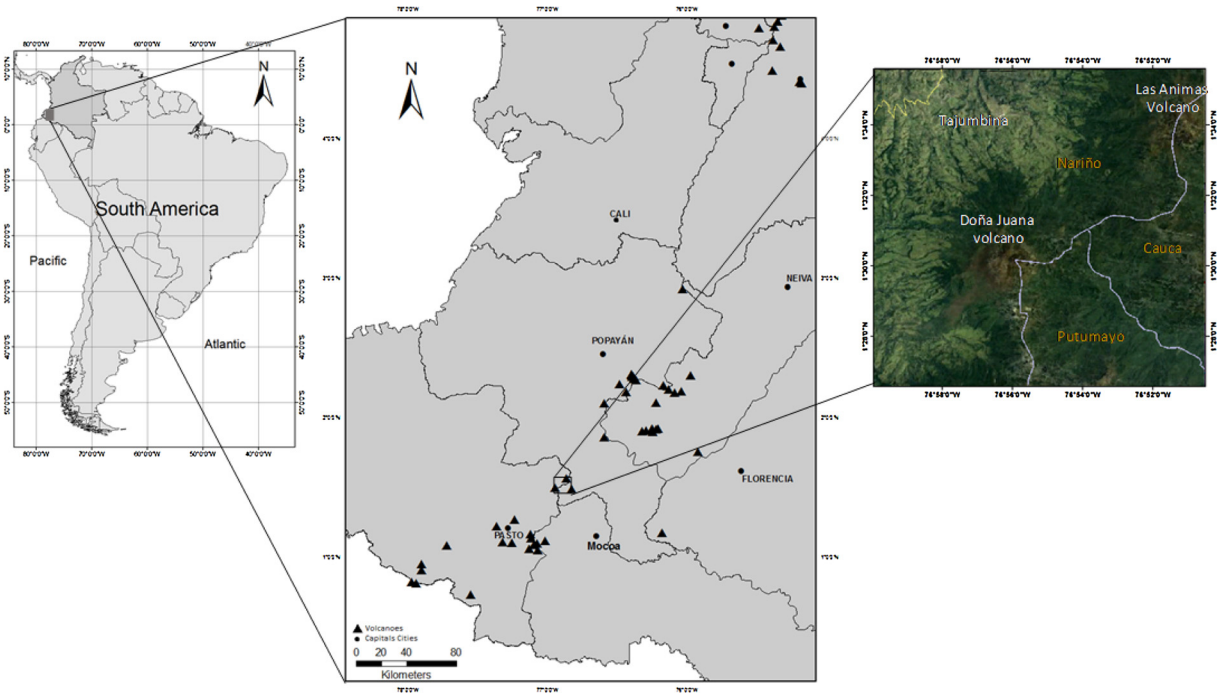

Fig. 1. Doña Juana Volcanic Complex (DJVC) location map.

2. Geological Setting

The basement of the Doña Juana complex is composed of Precambrian-Paleozoic metamorphic rocks, next to the cretaceous volcanic rocks of the Quebradagrande Complex through a fault contact (Fig. 2). The DJVC, is formed by several volcanic structures, (1) Santa Helena – caldera; (2) intra-caldera Doña Juana volcano ancient and the actual Doña Juana Volcano formed by numerous lava domes (Navarro et al., 2009).

The Doña Juana volcanic rocks consist mainly of dacites and andesites with some variations to basic andesites and basalts. In general, they present a seriate-texture with plagioclase, pyroxenes and amphibole phenocrysts, which show special corona reactions, complexes, zoning, sieve-texture, poikilitic-texture and embayed-texture. Microlites of plagioclase and interstitial glass matrices are also observed (Marín-Cerón et al., 2019).

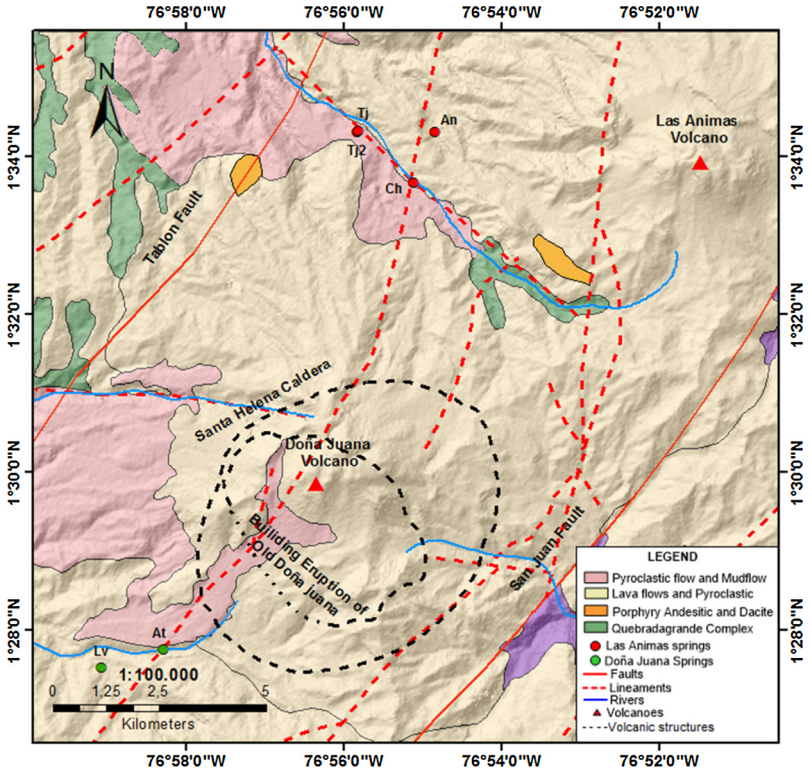

Fig. 2. DJVC Geological Map. Adapted and modified from geological map sheet 411-La Cruz (INGEOMINAS, 2002).

3. Methodology

3.1. Data and chemical balance

The chemical data for the DJVC thermal waters were obtained from the National Inventory of Hydrothermal Manifestations summarized by the Colombia Geological Survey, (SGC, 2019) at the website: http://hidrotermales.sgc.gov.co/.

The chemical analysis of samples from this site was performed in the SGC at their Water and Gas laboratory and the Stable Isotope Laboratory. The analytical techniques included: volumetric analysis, ion chromatography, UV spectrometry, atomic absorption and inductively coupled plasma techniques and for isotope analysis Off-Axis ICOS (Integrated Cavity Output Spectroscopy) high-resolution absorption laser spectroscopy. For the interpretation of water chemistry, it is important to realize that not all springs will yield reliable information about the conditions deep in the reservoir. Hence, hot or boiling chloride springs with a strong upflow experience the least contamination and are therefore most suitable for reservoir-related research (Nicholson, 1993).

In order to verify the reliability of the chemical analyses presented by the SGC, we tested the ionic balance (Eq. 2) to identify the ionic imbalances and analytical errors at the time of sample selection. If the results of the Charge Balance Error ion (CBE) exceed +/− 10%, they are not suitable for further geothermal studies (Nicholson, 1993). To calculate the CBE, the following solutes were used: Sodium (Na^+), Potassium (K^+), Calcium (Ca^{+2}), Magnesium (Mg^{+2}), Lithium (Li^+), Bicarbonates (HCO_3^-), Fluorine (F^-), Sulphate ($SO4^{-2}$), Chloride (Cl^-), compiled in Table 1.

$$CBE\% = \frac{\sum Cations - \sum Anions}{\sum Cations + \sum Anions} \times 100 \quad (2)$$

3.2. Fluid classification and geothermometry

The interpretation of the chemical data and the calculation of solute geothermometers was performed using the spreadsheet proposed by Powell and Cumming (2010).

The interpretation of geothermal water chemistry is best carried out on the basis of an initial classification, done in terms of the major cations and anions through a Piper and Tcsh plot (Cl-SO4 − HCO3). In order to know if the springs come from the same source, and to understand underground rock-gas interaction, we applied the Tclb (Cl-F-B) and Tcfb (Li-Cl-B) plots. Finally, to determine the cation water equilibrium, the Tnkm (Na-K-Mg) plot proposed by Giggenbach (1988) was used as a first approximation for reservoir temperature.

The solute geothermometers used were silica and cation geothermometers. Silica geothermometers are based on empirical formulas (Fournier and Potter, 1982). The chosen silica geothermometers were alpha cristobalite, chalcedony, quartz via conductive cooling and quartz adiabatic cooling (Table 1).

Seven different cation geothermometers were chosen based on different empirical formulas (Table 2). These included four different versions of the Na/K geothermometer (Truesdell, 1976; Fournier, 1979; Tonani, 1980 and Giggenbach, 1988), which yield temperature differences of 20–50 °C, the temperature range proposed for several empirical formulas by various authors, as well as the Na-K-Ca by Fournier (1981) and an Mg correction is also estimated with the method of Fournier (1981) and the K^2/Mg geothermometer by Giggenbach (1988).

Table 1
Silica geothermometer equations.

Silica Geothermometers	
Quarzt Adiabatic Fournier and Potter, 1982	$T°C = \frac{1522}{5{,}75 - Log(SiO2)} - 273{,}1$
Quartz Conductive Fournier and Potter, 1982	$T°C = \frac{1309}{5{,}19 - Log(SiO2)} - 273{,}15$
Chalcedony Fournier and Potter, 1982	$T°C = \frac{1032}{4{,}69 - Log(SiO2)} - 273{,}15$
Alpha Cristobalite Fournier and Potter, 1982	$T°C = \frac{1000}{4{,}78 - Log(SiO2)} - 273{,}15$

Table 2
Cation geothermometer equations.

Cation Geothermometers	
Na-K-Ca Fournier, 1981	$T°C = \frac{1647}{Log(Na/K) + \beta Log(\frac{\sqrt{Ca}}{Na}) + 2{,}24} - 273{,}15$ (< 100 °C if β = 4/3 and > 100 °C if β = 1/3)
Na-K-Ca Correct. Mg Fournier, 1981	Correction T.Na-K-Ca - TΔMg (Temp. Na-K-Ca > 70 °C and R < 50) (No mixing water)
Na/K Fournier, 1979	$T°C = \frac{1217}{1{,}438 + Log(\frac{Na}{K})} - 273{,}15$
Na/K Truesdell, 1976	$T°C = \frac{855{,}6}{0{,}8573 + Log(\frac{Na}{K})} - 273{,}15$
Na/K Giggenbach, 1988	$T°C = \frac{1390}{1{,}75 + Log(\frac{Na}{K})} - 273{,}15$
Na/K Tonani, 1980	$T°C = \frac{883}{0{,}78 + Log(\frac{Na}{K})} - 273{,}15$
K/Mg Giggenbach, 1988	$T°C = \frac{4410}{013{,}95 + Log(\frac{k^2}{Mg})} - 273{,}15$

The application of solute geothermometers depends on the temperature where the quartz geothermometers are suitable, which comprises temperatures above 150 °C. Chalcedony or α-cristobalite geothermometers are suitable for temperatures between 100 °C–150 °C. For temperatures below 100 °C, the amorphous silica geothermometer is recommended (Karingithi, 2009). Furthermore, the Na/K geothermometers are reliable for reservoirs with temperatures between 150 °C–200 °C. In the case of lower temperatures (< 150 °C), they can lose their usefulness, and the use of the K^2/Mg geothermometer, which is suitable under 150 °C, is recommended.

Finally, Na-K-Ca with and without an Mg correction were used. The Na-K-Ca is suitable for temperatures above 180 °C, and especially > 200 °C. However, this presents issues due to sensitivity to CO_2 concentration, especially at low temperatures (Pačes, 1975). Therefore, the Na-K-Ca with an Mg correction can be applied for cooler temperature systems and magnesium-rich waters, as suggested by Fournier and Potter (1979).

In order to apply mineral equilibrium geothermometry, it is necessary to identify the mineral phases in the geothermal fluid and saturation at predetermined temperatures to obtain a saturation index (log (Q/K)) using speciation program such as PHREEQC software. The saturation index values were plotted, against temperature for each mineral; which gave us an estimation of the equilibrium state of the fluid. The best estimate of the subsurface temperature can be regarded as the average equilibrium temperature indicated by many minerals, but only if these values are similar (D'Ámore and Arnórsson, 2000).

4. Dataset hydrogeochemical analysis

The results of chemical analysis of hot springs from the Doña Juana Complex are presented in Table 3. The waters were divided into two groups according to their location and concentration of dissolved solids: (1) the Doña Juana System (DJS) comprising La Vega (Lv) and Aguas Tibias (At); and (2) the Animas System (AS) constituting the Churos (Ch), Tajumbina I (Tj1), Tajumbina II (Tj2) and Animas (An). The table also presents the CBE% of the analyzed samples below ± 10%, hence the results for the spring waters are reliable and can be considered in further analyses.

Table 3
Major chemical constituents and percentage of CBE, $\delta^{18}O$ and δD isotope ratios of thermal waters from Doña Juana complex. The species of solution expressed in mg/l.

System	Sample	Temp C°	pH	Li	Na	K	Ca	Mg	SiO_2	B	Cl	F	SO_4	HCO_3	CBE%	δ18O	δD
DJS	Lv	24	6,31	0,40	51,20	5,10	33,30	18,70	72,64	0,28	36,87	0,90	155,03	107,36	−4%	−10,80	−70,72
	At	26	6,32	0,40	58,60	5,80	31,20	20,20	79,71	0,45	31,81	1,00	114,68	107,36	8%	−10,73	−70,13
AS	Ch	55	6,51	–	951	50,00	108,00	20,00	75,00	12,60	1276,88	0,72	151,98	1171,20	−8%	−8,90	−66,9
	Tj1	42	6,11	1,00	414	31,00	64,00	17,00	163,93	4,80	511,16	0,88	235,59	573,40	−9%	−9,96	−70,27
	Tj2	62	6,70	2,40	1168	79,20	158,00	32,20	226,07	14,80	1332,13	0,16	199,53	1964,20	−7%	−9,16	−68,13
	An	39	5,75	–	250,00	12,50	35,00	12,50	150,00	2,70	256,03	0,40	31,13	439,00	−4%	−10,16	−72,6

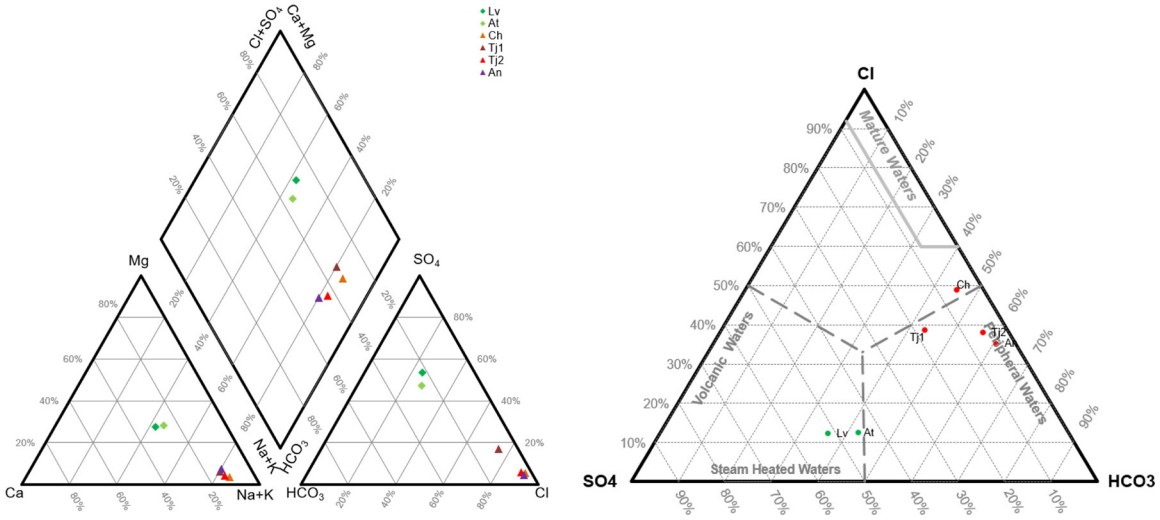

Fig. 3. Piper Plot in and Tcsh plot; DJS spring waters green dots and AS spring waters red dots. The Piper plot is in milliequivalent and the Tcsh is in ppm. The plots were made on a spreadsheet of Liquid Analysis v3 (Powell and Cumming, 2010).

4.1. Classification of the thermal springs

According to the Piper plot (Fig. 3), the DJS thermal waters are calcium sulfate waters (top quadrant), while the AS are sodium-chloride waters (right quadrant). A better visualization of the thermal water characteristics is shown by the Tcsh diagram. The Doña Juana System (Lv, At) waters plot between sulfate and bicarbonate waters, with a low chloride concentration and a low concentration of alkalis. The alkali concentrations are high but the chloride concentration is moderate in the Las Animas System waters, plotting close to the chloride axis, with the exception of the Churos spring, which plots on the chloride axis (Fig. 3).

The Tclb and Tcfb plots (Fig. 4) use the Cl, B, F, Li as tracers of water mixing, facilitating the identification of waters with a common origin. For example, the Li in the geothermal system is considered "conservative" despite being reactive, because at high temperatures it is highly mobile, whereas B is regarded as conservative because it only forms in soluble mineral and its sources of supply to the geothermal fluid are too limited to become saturated with any mineral (Arnórsson, 2000).

The Tclb diagram illustrates a low Li concentration and a high Cl/B ratio. The DJS samples plot just below the AS samples, showing a high chloride concentration and a similarity with the four springs; Tcfb presents a similar behavior. In general, two clusters are observed for the

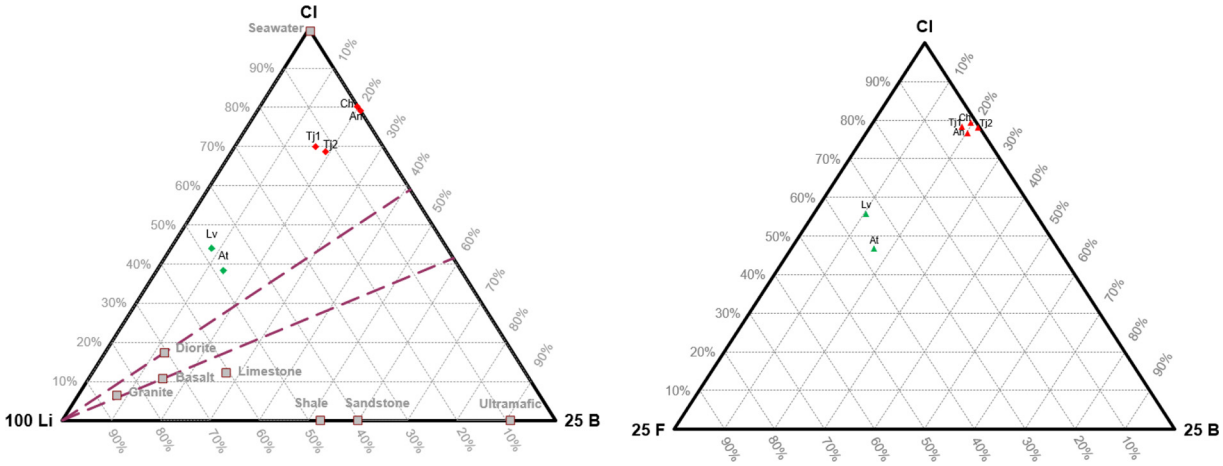

Fig. 4. Left Tclb Plot and right Tcfb Plot; DJS hot springs are represented by green dots and the AS system hot springs by red dots. The plots were made on a spreadsheet of Liquid Analysis v3 (Powell and Cumming, 2010).

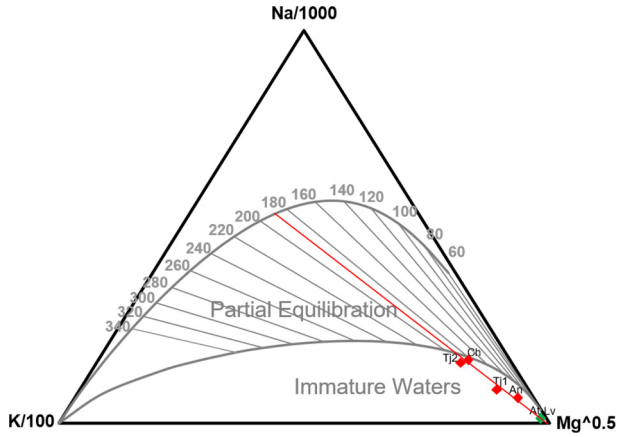

Fig. 5. Tnkm Plot; DJS spring waters are represented by green dots and the AS spring waters by red dots. Red line represents the temperature trend. The plot was made on a spreadsheet of Liquid Analysis v3 (Powell and Cumming, 2010).

influence zones determined by AS and DJS.

The Tnkm Plot (Fig. 5) shows that the DJS and AS waters are within the range of immature waters and although cation geothermometers should not be applied if the thermal waters are not in equilibrium, the spatial distribution of the springs nonetheless constitutes an important tool for understanding the system (Nicholson, 1993). Indeed, it is possible to note a trend toward partial equilibrium where the temperature is around 180 °C. Moreover, Tj2 and Ch are very close in partial equilibrium, hence by comparing different geothermometers it is possible find a relationship in waters less affected by mixing processes.

4.2. Solute geothermometers

To estimate the subsurface temperature, we used silica and cation solute geothermometers. Silica geothermometers are based on temperatures, depending on the solubility of different silica species (i.e., quartz, chalcedony, cristobalite, amorphous silica, etc.), in water as a function of temperature and pressure. Cation geothermometers are based on ion exchange reactions involving alkalis between the solutions' various alteration minerals. We have included the whole data set, although it is imperfect and may reflect temperature values that can be either overestimated or underestimated. Table 4 presents the results obtained by different silica geothermometers (Alpha cristobalite, chalcedony, quartz conductive, and quartz adiabatic) for both spring systems. Volcanic rocks such as basalts contain minerals that are dissolved relatively quickly, and consequently the low rate of quartz precipitation does not cope with the rate of silica released into the solution by the dissolving primary mineral, and the water tends to equilibrate with chalcedony (D'Ámore and Arnórsson, 2000), Consequently, chalcedony and alpha cristobalite were used for this research. The amorphous silica temperature was discarded along with β-cristobalite, because the temperature of amorphous silica is similar to the discharge temperature and β-cristobalite is stable at a very high temperature.

Table 4
Silica Geothermometers. Values in °C based on Fournier and Potter´s formulas (1982).

System	Sample	Alpha Cristobalite	Chalcedony conductive	Quartz conductive	Quartz adiabatic
DJS	Lv	69	92	120	118
	At	74	97	125	122
AS	Ch	71	93	122	120
	Tj1	117	144	167	157
	Tj2	139	169	189	175
	An	111	137	161	153

Table 5
Cation geothermometers. Values in °C; (1) Fournier, 1981, (2) Fournier, 1981, (3) Fournier, 1979, (4) Truesdell 1973, (5) Giggenbach, 1988 (6), Tonani, 1980, (7) Giggenbach, 1988.

System	Sample	Na-K-Ca (1)	Na-K-Ca Mg corr. (2)	Na/K (3)	Na/K (4)	Na/K (5)	Na/K (6)	K^2/Mg (7)
DJS	Lv	59	49	217	187	232	222	46
	At	66	41	216	186	231	222	48
AS	Ch	151	85	167	127	186	156	99
	Tj1	171	66	193	158	210	190	88
	Tj2	176	83	186	149	203	180	105
	An	105	53	164	123	182	151	70

The DJS temperatures ranged from 69 °C to 125 °C, while temperatures between 71 °C and 189 °C were suggested for the AS springs in Table 4. The temperature values by α-cristobalite and chalcedony geothermometers were the lowest (in the range of 75 °C to 144 °C), before values steeply increased with quartz adiabatic and conductive geothermometers in the range 120 °C–189 °C.

Table 5 shows the results for seven different types of cation geothermometers widely applied in geothermal exploration, i.e., four versions of Na/K geothermometers, Na-K-Ca, Na-K-Ca Mg correction, and K^2/Mg geothermometers. Temperatures between 41 °C and 232 °C were obtained for DJS waters, and temperatures between 53 °C and 210 °C for AS waters. The highest temperature in both systems were from the Na/K geothermometer by Giggenbach (1988), and the lowest by Na-K-Ca Mg correction by Fournier (1979).

5. Discussion

5.1. Evaluation of origin and mixing processes

Before interpreting the geothermometer data, it is important to understand the mixing processes, as the combination of geothermal fluids and cold water may yield misleading results (Arnórsson, 2000). The ^{18}O and ^{2}H isotope ratio make it possible to evaluate the origin of the waters using the stable isotope graph proposed by Giggenbach (1992), permitting the identification of factors of subsurface water mixing, water-rock interaction, and vapor separation processes.

The Fig. 6. shows the variation of δD and $\delta^{18}O$ in the geothermal waters collected in the survey zone where the red line represents Colombian Meteoric Line (CML) (Rodríguez, 2004) and in gray line is the Global Meteoric Water line (GWML). The thermal plot around these lines, with an oxygen shift toward the enrichment of oxygen from DJS to AS possibly being related to meteoric water mixing with geothermal fluids as suggested in the Figs. 7 and 8. The origin of the geothermal water appears to be predominantly precipitation, with Tj2 and Ch springs apparently less affected.

Through a positive linear relationship between the element concentrations of Cl and Na on the one hand, and SiO_2 with HCO_3 and SiO_2 on the other, may render the data regarding mixing reliable. Indeed, even a relationship between conservative elements such as Cl and $\delta^{18}O$ provides evidence of mixing (Arnórsson, 2000). Fig. 7 presents four diagrams that depict a linear relationship between Cl and other constituents, as well as a positive relationship between HCO_3 and SiO_2, where all plots suggest a predominance of the mixing process. However, the high ratio of chloride from Tj2 and Ch indicates that these waters could be cooling through conductive heat loss from deep hot waters.

5.2. Plot interpretation and geothermometer analysis

As previously mentioned, the DJS are sulphate waters with low Cl and alkali concentrations relative to AS (Fig. 3). In addition, the DJS anion concentration plot close to the steam-heated water range; the

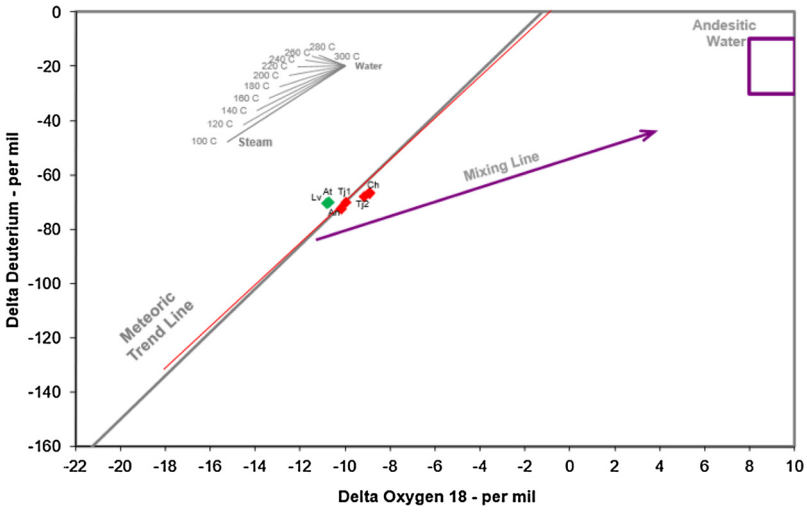

Fig. 6. Cross-plot of the stable isotopes of water (δ18O – δD). It includes the World Meteoric Trend line, the range of andesitic water as proposed by Giggenbach (1992). DJS spring waters are represented by green dots and AS spring waters are represented by red dots. The cross-plot was made on the spreadsheet of Liquid Analysis v3 (Powell and Cumming, 2010).

high HCO_3 could be either due to CO_2 vapor condensation of surface waters or CO_2 rich fluids with primary fluids as mentioned by Arnórsson et al. (2007), suggesting a mixing process as observed in the previous section. Meanwhile, the AS spring water anion concentration plot at the axis of bicarbonate waters with high concentrations of Cl and Na + K, and a pH close to neutrality, revealing a tendency toward maturity. Moreover, the AS waters are richer in dissolved solids than the DJS water, possibly indicating a greater interaction of thermal fluids and the host rock. In general, the interaction of thermal waters with hot, acidic magmatic gases develops favorable conditions for the leaching of cations and anions from host rock formations.

As mentioned before, the Tclb and Tcfb plots show two clusters for each zone. Apparently, all the springs from AS come from the same source, as well as the springs from DJS, but it is not totally certain whether the springs of DSJ and AS share the same reservoir. This is observed in the ratio diagram for chloride, boron and lithium (Fig. 8). The plot shows a clear positive correlation (R^2 = 0,99) of the Cl/B ratio, suggesting a common reservoir for the AS. At the same time, the Cl/B

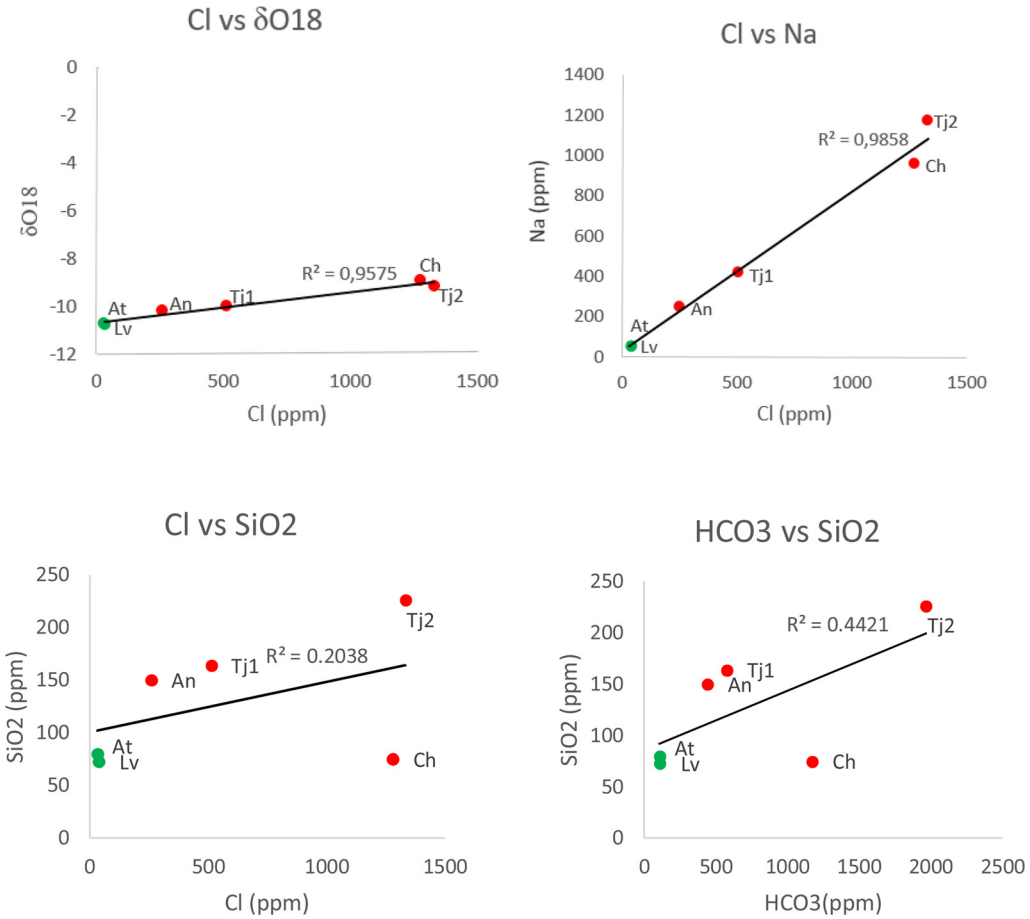

Fig. 7. Cl vs δ^{18}O, Cl vs Na, Cl vs SiO_2 and HCO_3 vs SiO_2 for Doña Juana Complex. Doña Juana system spring waters are represented by green dots and Las Animas system spring waters by red dots. The R2 values with ratios around 0,9 indicating a good fit of the model to the data.

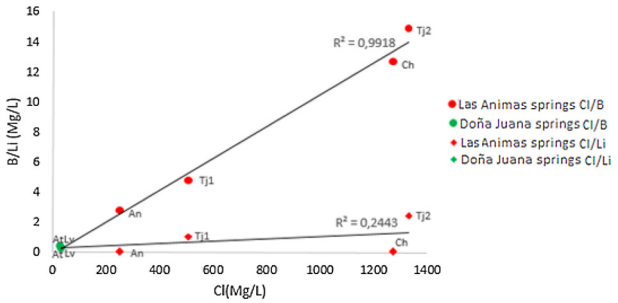

Fig. 8. Cl/B and Cl/Li ratios for DJS spring waters and AS spring waters. The R2 values for Cl/B ratios are around 0.9 indicating a good fit of the model to the data.

manifests similar behavior as the ratio diagrams provide more evidence of mixing processes. In contrast, the Cl/Li ratios reveal a weak linear correlation ($R^2 = 0,24$), potentially due to the absence of Li from Animas and Churos springs in the samples, thus complicating data interpretation.

The strong correlation between B and Cl concentrations in the AS waters implies a single reservoir. This may be an indicator of vapor absorption by magmatic gases, and hence an older hydrothermal system due to the loss of boron; another possibility is related to the boron lost from the adsorption by clays during lateral flow. Considering the temperature, distance and concentrations of conservative elements and alkalis, the different Cl/B ratio of DJS and AS appears to be due to element adsorption by the lithology in the lateral flow. Therefore, we can infer that the upflow zone is at the AS and the outflow zone is at the DJS.

In general, waters from both systems (DJS and AS) can be classified as immature because they have not yet reached equilibrium (see Fig. 5), due to the fact that they are mixed with cold groundwater. Therefore, it is not possible to estimate the temperature of the reservoir with absolute certainty, and therefore both systems (DJS and AS) are unsuitable for the application of some solute geothermometers. However, this plot shows a trend toward the equilibrium line, most likely indicating a reservoir at equilibrium with a temperature above 180 °C.

The solute geothermometers yield several values where DJS indicates problems, as expected. The values for AS spring waters appear to be suitable for analysis, with the exception of that from the Churos spring, which is problematic for the silica geothermometers, probably due to dilution. After comparing and correlating both solute geothermometers, the AS waters show a temperature range of between ~160 °C - ~200 °C for Tj1 and Tj2 through high-temperature geothermometers such as quartz, Na/K and Na-K-Ca. Nevertheless, the An and Ch spring waters suggest lower temperatures than those of Tj1 and Tj2 when applying the same geothermometers between ~105 °C and ~180 °C, suggesting that they have been profoundly affected by mixing and thus yield misleading temperatures. The Na/K and quartz geothermometers probably indicate the temperature of a deep reservoir above 150–190 °C for AS, and they are the most reliable because their values are close to each other and are suited to this temperature range.

On the other hand, when the waters ascend, they may interact with secondary minerals and consequently reach equilibrium with minerals at low temperature (~80 °C to ~120 °C), as determined by geothermometers using Mg and K^2/Mg corrections. Nevertheless, these temperatures remain doubtful, as is the case with K^2/Mg geothermometers, because they are so sensitive to mixing waters. We opted to explore mineral equilibrium geothermometry (Fig. 9) as a proxy for validation, and to identify the mineral equilibria. Nevertheless, the Tj1, An and Ch water samples were discarded because they appeared to be more significantly affected, generating a simple shift and a displacement of the mineral log (Q/K) toward lower temperatures (Pang and Reed, 1988). Consequently, Tj2 was the only sample suitable due to its accordance with the temperature estimated using silica quartz, Na-K, and Na-K-Ca converge towards 170–190 °C suggesting this water is less affected by mixing with surficial waters (especially, the silica concentration).

The hydrothermal alteration for mineral equilibrium geothermometry were chosen regarding the geology of the survey zone. Given that the aluminum concentration is lower than the limit of quantification for the sample, it was calculated forcing equilibrium with K-feldspar and being controlled at 180 °C. The Saturation index (SI) of each species was identified using the PHREEQC program where the range of temperature was limited from the discharge temperature at the surface and up to 200 °C, one of the maximum values estimated by geothermometers.

According to Pang and Reed (1988), these curves of different slopes reflect their thermodynamic characteristics. Therefore, the indication of a possible equilibrium should be more reliable if the minerals that converge on the zero log(Q/K) line are of different types. Accordingly, the Tajumbina II water revealed an association at around ~180 °C, as quartz, chalcedony, anhydrite, ca-momorillonite, albite and illite converged with quartz adiabatic, Na-K and Na-K-Ca geothermometers (Fig. 9). Consequently, Tj2 appears to be the most representative sample of the deep reservoir fluid at 180 +/− 20 °C.

5.3. Conceptual model

According to these findings, the heat source of the geothermal system could be a young magma chamber from the Doña Juana and Las Animas volcanoes, where the regional Romeral fault system permitted the geothermal fluids to ascend. As has been described, the volcano-sedimentary rocks of the Quebradagrande complex mainly form the basement in this volcanic zone. The overlying Neogene pyroclastics and Quarternary deposits may act as a seal rock where the mixing processes takes place.

The geothermal fluids appear to flow through the fault structures, and permeable zones play an important role in the vertical permeability of the geothermal system. At the same time, this may be facilitated by the secondary-permeability of the Quebradagrande Complex for storing and transporting water. On the other hand, the conceptual model (Fig. 10) shows an intersection between normal faults and transverse oblique-slip faults around the AS, where multiple minor faults typically connect major structures and fluids, hence the fluids can flow readily through highly fractured dilational quadrants (Fauld, 2015).

The sodium-chloride waters of the AS originate in the interaction of geothermal fluids with the host rock and dilution with low-salinity shallow waters. The relative concentration of conservative and tracer ions suggests that the DJS waters can be considered a part of the same reservoir, being the outflow zone. Therefore, the differences in the concentrations of these elements may due to diminishing adsorption of elements in the lateral flow.

Finally, the relationships between $\delta^{18}O$ and $\delta^{2}H$, Cl concentration and $\delta^{18}O$, Na and B concentrations indicate mixing of meteoric water and geothermal fluids, with condensation from magmatic gases. Regarding the geothermometry results taking, saturation index and structural geology into consideration, the AS zone is the best area for geothermal exploration, related to a high temperature system (> 150 °C).

6. Conclusions

The geochemical characterizations of the thermal springs in the Doña Juana Complex can be summarized as follows:

The water types in the DJVC are dilute chloride waters (Las Animas system) and bicarbonate sulfate waters (Doña Juana system). The concentrations of “conservative” elements in this study, such as Cl, Li and B, as well as the $\delta^{18}O$ values did not permit the identification of a clear relationship between the reservoirs of DJS and AS. However, they may belong to the same reservoir and the difference between the Cl/B ratio could be due to the adsorption of B by clay minerals in the lateral

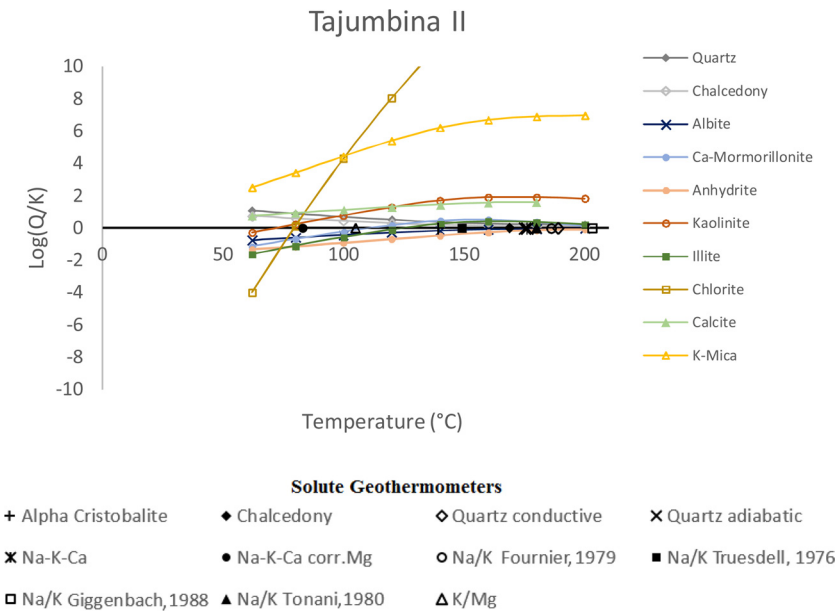

Fig. 9. Saturation index (log Q/K) vs. temperature for AS spring waters calculated with PHREEQC. Solute geothermometers added on X axis at 0 for comparing with the temperature estimated in the mineral assemblage.

flow.

The results of isotope analysis and different relationships of chloride concentrations with other component concentrations suggested mixing between geothermal fluids and meteoric waters, where the Tj2 thermal water is less affected by mixing processes, suggesting that its data are the most reliable, indicating strong correlations between quartz, Na-K-Ca and Na/K geothermometers (170 °C–190 °C).

The most suitable geothermometers are quartz conductive and Na/K geothermometers because they yield a similar temperature range. In addition, Na/K geothermometers are less affected by dilution and steam separation, unlike K2/Mg or Na-K-Ca. In general, the correlation between some geothermometers and the mineral equilibrium geothermometry of TJ2 sample demonstrates a mineral equilibrium phase at around 180 °C related to a deeper reservoir.

Finally, it is evident that the hot springs of the zone surveyed represent the product of the mixing of gases and conductive heat from the

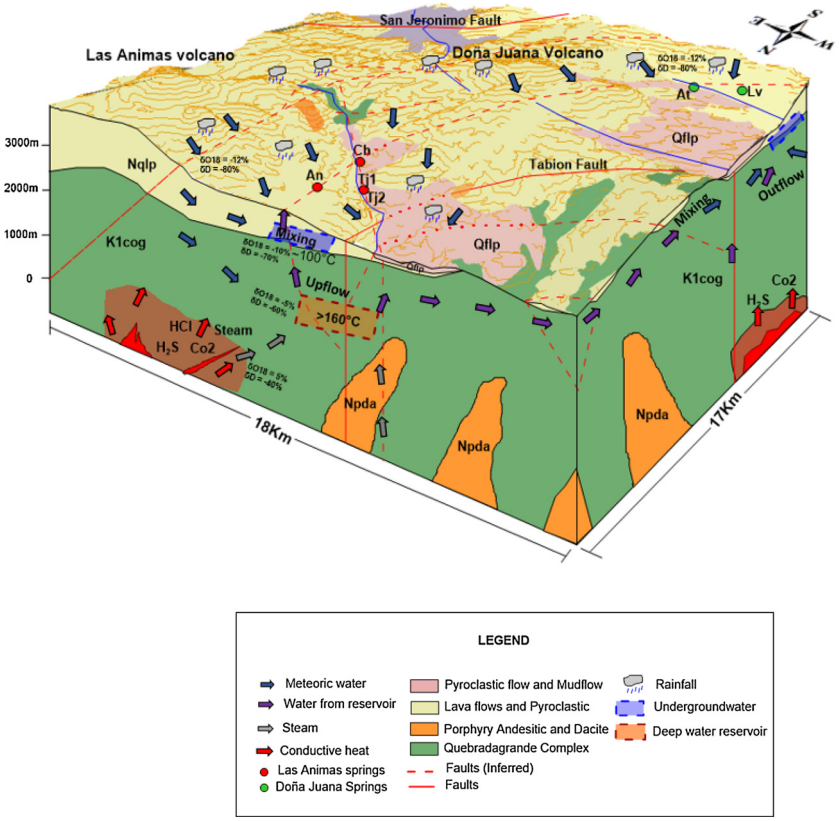

Fig. 10. The conceptual model of the Doña Juana complex system based on surface geology and hydrogeochemical characterization.

Doña Juana Complex. Indeed, the gases interact with AS fluids (upflow zone), which are recharged by meteoric waters, before being infiltrated at the fracture zone along with the condensation of gases. The intersection of fault systems may play an important role in permeability control, increasing the geothermal potential to the northwest of the Doña Juana volcano, and suggesting a high temperature geothermal system (170 °C to 190 °C).

Declaration of Competing Interest

None.

Acknowledgements

The authors thank the EAFIT University's Research Direction for their support in the consolidation of the geothermal research line. Special thanks to Ana M. Contreras for her valuable support, and to the Geological Colombian Survey for sharing the data through the National Inventory of Hydrothermal Manifestation. The authors are grateful to the editor Dr. Halldor Armannsson and the anonymous reviewers for their invaluable comments which helped to improve the content of this paper.

References

Arnórsson, S., 2000. Mixing process in upflow zones and mixing models chapter 11 (pp. 200-211) in S. Arnórsson (2000) isotopic and chemical techniques in geothermal exploration, development, and use. Sampling Methods, Data Handling, Interpretation. International Atomic Energy Agency, Vienna, pp. 152–199.

Arnórsson, S., Stefánsson, A., Bjarnason, J., 2007. Fluid-fluid interactions in geothermal systems. Rev. Mineral. Geochem. 65 (1), 259–312.

D'Ámore, F.D., Arnórsson, S., 2000. Geothermometry. In: Arnórsson, S. (Ed.), Isotopic and Chemical Techniques in Geothermal Exploration, Development and Use. Sampling Methods, Data Handling, Interpretation. International Atomic Energy Agency, Vienna, pp. 152–199.

Fauld, J.E., 2015. Favorable tectonic and structural settings of geothermal systems in the Great Basin region, Western USA: proxies for discovering blind geothermal systems. Proceedings World Geothermal Congress. 19–25.

Fournier, R.O., 1979. A revised equation for the Na/K geothermometer. Geothermal Resources Council Transactions. pp. 1–16 5.

Fournier, R.O., 1981. In: Ryback, Muffler (Eds.), Application of Water Geochemistry to Geothermal Exploration and Reservoir Engineering in Geothermal Systems: Principles and Case Histories. John Wiley and Sons, New York, pp. 109–143.

Fournier, R.O., Potter, R.W., 1979. Magnesium correction to the Na-K-Ca geothermometer. Geochim. Cosmochim. Acta 43, 1543–1550.

Fournier, R.O., Potter, R.W., 1982. A revised and expanded silica (quartz) geothermometer. Geoth. Res. Council Bull. (November), 3–12.

Giggenbach, W.F., 1988. Geothermal solute equilibria. Derivation of Na-K-Mg-Ca. Geochim. Cosmochim. Acta 52 (12), 2749–2765.

Giggenbach, W.F., 1992. Isotopic shifts in waters from geothermal and volcanic systems along convergent plate boundaries and their origin. EPSL 113, 495–510.

INGEOMINAS, 2002. Geological Map La Cruz (Sheet 144, 1:100.000). Cauca, Nariño and Putumayo deparments: INGEOMINAS (Colombia Geological Survey).

Karingithi, C.W., 2009. KenGen and GDC, at Lake Naivasha, KenyaChemical Geothermometers for Geothermal Exploration Presented at Short Course Lv on Exploration for Geothermal Resources, Organized by UNU-GTP2009. Chemical Geothermometers for Geothermal Exploration Presented at Short Course Lv on Exploration for Geothermal Resources, Organized by UNU-GTP 1–22.

Marín-Cerón, M.I., Leal-Mejía, H., Bernet, M., Mesa-García, J., 2019. Late cenozoic to modern-day volcanism in the Northern Andes: a geochronological, petrographical, and geochemical review. In: Cediel, F., Shaw, R.P. (Eds.), Geology and Tectonics of Northwestern South America. Frontiers in Earth Sciences. Springer, Cham, pp. 603–648.

Navarro, S., Pulgarín, B., Monsalve, M.L., Cortés, G.P., Calvache, M.L., Pardo, N., Murcia, H., 2009. Doña juana volcanic complex (DJVC), nariño: geology and eruptive history. Boletín de Geología 31 (2), 109–118.

Nicholson, K., 1993. Geothermal Fluids: Chemistry and Exploration Techniques. Springer Verla, Berlin.

Pačes, T., 1975. A systematic deviation from the Na-K-Ca geothermometer below 75°C and above 10-4 atm PCO2. Geochim. Cosmochim. Acta 29, 541–554.

Pang, Z.H., Reed, M., 1998. Theoretical chemical thermometry on geothermal waters: problems and methods. Geochim. Cosmochim. Acta 62 (6), 1083–1091.

Powell, T., Cumming, W., 2010. Spreadsheets for geothermal Water and gas geochemistry. Proceedings, Thirty-Fifth Workshop on Geothermal Reservoir Engineering 4–6.

Reed, M.H., Spycher, N.F., 1984. Calculation of pH and mineral equilibria in hydrothermal water with application to geothermometry and studies of boiling and dilution. Geochim. Cosmochim. Acta 48, 1479–1490.

Rodríguez, C., 2004. Línea meteórica isotópica de Colombia. Meteorol. Colomb. 8, 43–51.

SGC, 2019. Base De Datos De Inventario Nacional De Manifestaciones Hidrotermales De Colombia. Grupo Exploración de Recursos Geotérmicos. http://hidrotermales.sgc.gov.co/invtermales/.

Tonani, F., 1980. Some remarks on the application of geochemical techniques in geothermal exploration. Proceedings, Adv. Eur. Geoth. Res., Second Symp., Strasbourg. pp. 428–443.

Truesdell, A., 1976. Summary of section III: geochemical techniques in exploration. Proceedings 2nd U.N. Symposium on the Development and Use of Geothermal Resources.